AN EXAMINATION OF THE 12 JUNE 2004 MULVANE, KANSAS TORNADO

Scott F. Blair[1*] and Eric M. Nguyen[2]

[1]Atmospheric Sciences, University of Louisiana at Monroe, Monroe, Louisiana
[2]School of Meteorology, University of Oklahoma, Norman, Oklahoma

1. INTRODUCTION

An active severe weather event transpired across the central plains during the afternoon and evening hours of 12 June 2004. Most notably, a single tornadic supercell thunderstorm produced several tornadoes that struck parts of southern Kansas (Fig. 1). The strongest of these tornadoes affected the outskirts of Mulvane, Kansas producing at least high-end F3 damage to property and vegetation. This tornado was on the ground for 12 minutes (0021 UTC – 0033 UTC) consisting of a 6.4 km path length and a maximum width of 0.45 km. The most notable damage occurred during the latter duration of the tornado where a well-structured two-story house was demolished. A vehicle inside the garage was ejected 251 m away from the house. Total damage estimates associated with this tornado totaled $575,000 dollars, along with 2 injuries and 1 livestock fatality.

2. SYNOPTIC SCALE ENVIRONMENT

On the morning of 12 June 2004, the setup for potentially tornadic supercells appeared to exist from western Oklahoma to southeast Nebraska. At 1200 UTC, a

* *Corresponding Author Address:*
Scott F. Blair, University of Louisiana at Monroe, Monroe, LA 71209
E-mail: scott10@flash.net

shortwave trough was present over the southern plains allowing for morning convection to develop over parts of central and northern Kansas. Further east into Missouri, a mesoscale convective system (MCS) was ongoing from overnight convection which continued to increase in both coverage and intensity throughout the day. This MCS was associated with synoptic scale forcing caused by the initial shortwave trough and upper level divergence. Further west, a much stronger shortwave trough was located west of the four-corners region associated with an almost neutrally tilted longwave trough. 500mb winds were generally weak to moderate over the plains with winds averaging 10-15 ms^{-1} at 1200 UTC. An 850mb low was centered over southwestern Kansas, with a strong isodrosothermal gradient stretching from Lubbock, Texas into western Oklahoma and through central Kansas. Surface winds ranged from 5-15 ms^{-1} out of the south and southwest over most of the southern plains. A 1009mb surface low was located southwest of Dodge City, Kansas (DDC) with a dryline extending southward through the Oklahoma Panhandle and the eastern Texas Panhandle. A warm front extended northeast of the surface low across central Kansas stretching into southeast Nebraska. A northwest-to-southeast oriented outflow boundary stretched from the dryline in northern Kansas to the ongoing MCS in southern Missouri.

As the day progressed, the surface low deepened and propagated northeast in response to persistent pressure falls in the vicinity of Hays, Kansas. By 2000 UTC, the surface low deepened to around 1006mb with surface temperatures reaching 310 K near the surface low extending southward into western Texas, generally west of the dryline. As the dryline mixed east, surface winds gradually increased from about 3-5 ms^{-1} at 1200 UTC to 10-13 ms^{-1} over southern and central Kansas at 2000 UTC. Convection rapidly developed in the vicinity of the dryline over northwestern Oklahoma into central Kansas where convective temperatures were reached. By 2200 UTC, the dryline stalled just east of Pratt, Kansas and slowly began to retrograde back to the west as indicated on both the surface and radar observations (Fig. 2). The intense convection that developed in southern Kansas rapidly moved east leaving a well defined outflow boundary that was observed by the authors. When the Mulvane, Kansas supercell was in the vicinity of this boundary, rapid intensification was observed on radar. This boundary had a much lower lifted condensation level (LCL) then the ambient environment, backed surface winds which allowed stronger storm relative helicity to be present, and possibly provided the source for streamwise vorticity aiding in tornadogenesis (Markowski et al. 1998; Atkins et al. 1999).

By 0000 UTC, the system aloft became negatively tilted and was located over the high plains (Fig. 3). 500mb winds over southern Kansas had increased from roughly 10 ms^{-1} to about 15 ms^{-1} observed at Lamont, Oklahoma (LMN), approximately 100 km south of the Mulvane, Kansas tornado. The combination of steep lapse rates, surface dewpoints reaching 294-297 K, and strong daytime heating resulted in convective available potential energy (CAPE) values exceeding 4000 JKg^{-1}. Throughout the rest of the evening, the cluster of severe storms associated with the Mulvane, Kansas tornado moved east and later merged with a fast moving derecho that developed with a cluster of storms in northeast Kansas. This resulted in a widespread wind event over much of eastern Kansas and western Missouri as the derecho rapidly moved southward, reaching northeastern Oklahoma by 0700 UTC.

3. MESOSCALE ENVIRONMENT AND RADAR ANALYSIS

Fine line echoes from the Weather Surveillance Radar 88 Doppler (WSR-88D) in Wichita, KS (ICT) allowed for detailed analysis during the afternoon and evening hours. These echoes allowed for helpful dissection of the evolution of mesoscale events where large regions of sparsely populated observations hindered detailed surface analysis.

Three main surface features were noted on the WSR-88D prior to convective initiation and throughout the event (Fig. 4). A dryline was moving eastward throughout the afternoon hours and initiated convection in western Harper County. Roughly 80 km to the east of the dryline, a well-pronounced confluence line was located across western Sedgwick and western Sumner Counties and was slowly progressing westward. A large region of horizontal convective rolls (HCR) was noted to the east of the confluence line. The initial convection near the dryline rapidly blossomed and organized into an isolated supercell (SUP1) near Harper, Kansas. As SUP1 approached the

confluence line, base reflectivity decibels of Z (dBZ) and size gradually decreased. Reaching the confluence line, SUP1 took upon the appearance of a decaying supercell with continually decreasing reflectivity size. Other isolated convection initiated east of the storm, 16 km south of ICT and south of Wellington, Kansas near the state line. It is possible this convection initiated partially due to the close proximity of the confluence region and in response to the HCR present across the area. The correlation between HCR and convective initiation has been documented in literature (Edwards et al. 2000). Immediately crossing the confluence line, SUP1 rapidly increased in dBZ and overall organization. The convection immediately to the east of SUP1, now oriented east-northeast, also continued to increase in dBZ and size. SUP1 quickly became a well-organized supercell and changed its motion from 250 degrees to 270 degrees with much slower forward speed. A mesocyclone developed with SUP1 and a "hook echo" appendage evolved just west of Interstate 35. Other significant features developed at this time across the south-central Kansas region. Convection just east of Wellington, Kansas, approximately 48 km southeast of SUP1, produced a left-split supercell (LS1) with the motion from 225 degrees at 22 ms^{-1}. The convection east-northeast of SUP1 produced an outflow boundary that stretched across northern Sumner and Cowley Counties. Lastly, a rear-flank downdraft (RFD) boundary was noted west-southwest of SUP1 trailing into the updraft region. Satellite imagery from 2325 UTC shows a well-developed supercell characterized by a large overshooting top and anvil. In addition, LS1 is also visible just south of the anvil.

Throughout the 0000 UTC to 0031 UTC timeframe, SUP1 took upon a classic supercell appearance (Lemon and Doswell 1979) with a well-defined RFD boundary, forward-flank downdraft (FFD) boundary, and a persistent well-formed hook echo. Two additions to complicate this classic model include the SUP1 interaction with the preexisting outflow boundary from downstream convection and the ingestion and collapse of the LS1. Detailed analysis was performed during the 0014 UTC – 0036 UTC duration to examine the mesoscale environment before, during, and after the tornado. As the LS1 crossed the preexisting outflow boundary southeast of Udall, KS, base reflectivity dBZ pulsed. Once crossing the boundary at 0014 UTC, LS1 reflectivity quickly lowered indicating the beginning of dissipation stage. By 0018 UTC, the outflow boundary began to accelerate southward, perhaps in response to the collapsing LS1. The examined tornado in this study developed at 0021 UTC with a classic radar structure. SUP1 reached its peak "textbook" organization at 0027 UTC (Fig. 5, Fig. 6), and fully ingested the remnants of LS1. By 0036 UTC, the storm lost its classic appearance and base reflectivity dBZ values decreased. After the disorganization in appearance, SUP1 failed to produce any other tornadoes during the next 52 minutes.

Cross-sectional radar analysis was also preformed during the 0014 – 0036 UTC period. It has been noted that a correlation exists between the bounded weak echo region (BWER) height and tornadogenesis (Lemon et al. 1978; Lemon and Doswell 1979). Lemon noted in several case studies that a decrease in BWER height correlated to tornado touchdown several minutes after the reflectivity lowering. This principle relates to the cross-sectional analysis findings associated with the Mulvane, Kansas supercell characteristics. From 0014 –

0018 UTC, the supercell contained a well-formed BWER (Fig. 7). By 0023 UTC, a partial collapse of the BWER was evident and already underway as reflectivity lowered and slightly filled inward. The reflectivity height continued to progressively lower from 0027 – 0036 UTC, exhibiting further relative disorganization of the updraft (Fig. 8). The analysis suggests the BWER began to collapse several minutes before tornado touchdown, perhaps signifying a correlation that aided in the production of the Mulvane, Kansas tornado.

It is hypothesized the interaction of LS1 and the outflow boundary orientation aided in the decay of the tornado and disruption in organization of SUP1. Left-split supercells have been documented to create a disorganizing effect on the merger between left and right moving supercells (Lindsey and Bunkers 2004). LS1 moved over the upstream inflow region and later was ingested by SUP1. It was shortly after this period SUP1 experienced some disorganization. Radar data suggests the outflow boundary began to move south shortly after LS1 crossed the boundary. With the collapse of LS1 north of the boundary, it is possible the downdraft air aided in a southward surge of the outflow boundary. This eventually led to modifying the majority of pure inflow air into SUP1.

4. LIGHTNING DATA

There have been a number of observations to correlate cloud-to-ground (CG) lightning with the prediction and evolution of tornadoes (MacGorman and Nielsen 1991; Perez et al. 1997; Bluestein and MacGorman 1998). Similar observations were made to this case study to observe the lightning activity and its potential relationship to tornadogenesis and tornado duration.

Lightning data was collected from the National Lightning Detection Network (NLDN) for the duration of one hour, beginning and ending at 0000 UTC to 0059 UTC respectively. The range was limited to a 40 km diameter region centered on the supercell to prohibit other lightning activity to enter the database. In addition, the data was parsed into a twelve minute period (0021 UTC – 0033 UTC) during the time of the tornado. Lastly, the data was then mapped with Geographic Information System (GIS) software to determine the strike location in relation to the supercell.

It was discovered that the CG flash rate during the one hour period totaled to 374 flashes (Fig. 9). An interesting correlation arose to the activity of flashes per minute related to tornado time. Previous to tornadogenesis (0000 UTC – 0020 UTC), the average flash rate was on the order of 5 strikes per minute. It was found that lightning activity markedly rose just after tornadogenesis and persisted until three minutes after tornado dissipation. During the time of the tornado, the peak flash rate period sampled contained a strike rate average of 12 flashes per minute, more the double the amount of recorded lightning activity previous to the tornado. The tornado duration totaled 150 flashes, which contained 40% of all flashes in the entire hour sampled. The one minute flash maximum occurred at 0027 UTC with 27 flashes recorded. After 0036 UTC, lightning activity dramatically decreased to just under an average of 4 flashes per minute.

While not a direct indicator of tornado prediction, a significant correlation does exist with the dataset associated with lightning activity related to tornadic activity with this example. The forces resulting in

such a correlation may not entirely depend on the tornado, but instead focus on other processes occurring during the time of the tornado associated with the supercell. Although documentation exists where the total flash rate increases in tornadic storms near the time of the tornado (MacGorman et al. 1989), other physical storm characteristics are hypothesized to aid in the increase of flash rates per tornado duration. It was also shown that intensifying updrafts may reduce CG flashes by raising the negative charge centers needed for the production of CG lightning. This alters the height of the negative charge in the cloud, therefore reducing the flash potential. In addition, MacGorman et al. (1989) showed a relationship between the frequency of lightning flashes and the strength of the updraft. It was also shown that ground flash rates increased as reflectivity cores descended to lower heights.

Considering the aforementioned literature in relation to the cross-sectional radar analysis of the supercell near Mulvane, Kansas, it is hypothesized the stages of updraft strength were at least partially responsible for the lightning characteristics found within the dataset. During the time previous to tornadogenesis, lightning activity was rather low. Radar data shows a well-organized and intensifying updraft. At the time of tornadogenesis, radar shows signs of updraft weakening and the beginnings of the partial collapse of the BWER. Throughout the tornado duration, the reflectivity region began to descend towards the ground. It is hypothesized that the partial collapse of the BWER and the lowering of the reflectivity region allowed for the production of an active lightning flash period as negative charges were thought to be lower to the ground. Shortly after tornadogenesis, the supercell

was notably lesser in updraft organization and this is speculated to have resulted in the dramatic decrease in lightning production.

The location of CG strikes related to the supercell resulted in both normal and abnormal findings. As expected, a large amount of strikes were recorded within the precipitation region. However, large concentrations of strikes were noted in precipitation free (surface) regions, most notably near the mesocyclone and just south of the mesocyclone (Fig. 10). Traditionally, this is a region that does not experience a high volume of CG activity. The authors also observed many cases of "staccato" flashes in the rain free regions as described by Bluestein and MacGorman (1998). It is speculated that the active flash region near and just south of the mesocyclone is partially responsible to the lowering of reflectivity values associated with the BWER.

5. MOBILE DATA ANALYSIS AND RESULTS

Mobile surface observations were collected during the times before, during, and after tornado occurrence. The mobile observations were acquired by a "mobile mesonet" type vehicle, with specifications similar in design to Straka et al. (1996) with modern upgraded equipment where available. High temporal and spatial resolution data was obtained nearby and under the mesocyclone, which provides insight to several meteorological processes. Most importantly of these processes, data was collected and analyzed from the RFD of the supercell throughout the tornado lifespan. During this period, data was collected within close proximity of the tornado, allowing for an in-depth analysis of the thermodynamics and kinematics

associated with the RFD close to the tornado.

a. Mobile Surface Observations Overview (0000 – 0100 UTC)

Surface observations across south-central Kansas are relatively widely spaced. Therefore mobile surface observations collected, served as the principle data analyzed. With the main interest time that of the Mulvane, KS tornado (0021 UTC – 0033 UTC); the data set was focused on a range from 0000 UTC – 0100 UTC to acquire a solid understanding of the overall environment leading to, during, and after tornadogenesis (Fig. 11).

The thermodynamic environment north of the supercell near Wichita, Kansas (ICT) was characterized with temperatures (T) around 301 K and dewpoint temperatures (Td) around 291 K. As the vehicle traversed through the main precipitation core, T/Td markedly dropped to the lowest values recorded during the hour period. Once south of the main precipitation, T/Td rose and held at a steady value throughout the tornado duration, noting the exception of small fluctuations, with T averaging 299 K and Td averaging 295 K. The mobile vehicle then crossed into the base state storm inflow (BSSI) and the outflow boundary after tornado dissipation. T rose into the 300 K range and Td decreased into the 293 K range, which led to the end of the sample period. The kinematic transect through the supercell originated with southerly winds north of the supercell. The winds generally backed during the entire hour duration, eventually making a 360 degree span within the sample period.

b. Mobile Surface Observations Tornado Duration (0021 – 0033 UTC)

Mobile surface observations were acquired every 5 seconds underneath the mesocyclone. To prevent small timescale fluctuations and surface roughness anomalies, the data was averaged per 30 seconds and 1 minute timescales. All data collected was within 1.5 km or less of the tornado location.

The thermodynamics immediately north of the tornado track was characterized by T 1 K increase and Td 0.5 K lowering (0021 UTC - 0025 UTC). This is hypothesized to be in response to the narrow region of warm inflow wrapping around the north side of the mesocyclone. The kinematic wind field sustained winds from the northeast around 4.5 ms^{-1} north of the tornado track.

The tornado crossed the road at 0026 UTC within 0.4 km from the mobile vehicle. Shortly after, strong northwest winds sustained at 15 ms^{-1} marked the RFD boundary passage (Fig. 12). T decreased 1 K while Td increased 0.5 K during 0027 - 0029 UTC. Winds slowly backed south of the tornado track until 00:28:30 UTC when a north-northwest 30-second sustained wind of 20.1 ms^{-1} with gusts to 25.5 ms^{-1} was noted. This 30 second period contained the strongest sustained wind and gust recorded during the entire tornado lifespan. The winds then veered from 0029 UTC to 0031 UTC. Considering such a strong wind gust, it is suggested this feature marks another RFD passage or "surge" as documented in other studies (Finley and Lee 2004). The wind field also suggests this strong downdraft moved in an east-southeast direction, just north of the mobile vehicle, resulting in the observed veered winds recorded.

c. RFD Analysis (0021 – 0033 UTC)

With the close proximity of the RFD passage in relation to the mobile vehicle, an in-depth analysis can be preformed using several techniques to examine the thermodynamic characteristics of the RFD. Markowski et al. (2002) found RFDs associated with tornadic supercells contain surface equivalent potential temperature (Θe), virtual potential temperature (Θv), and convective available potential energy (CAPE) values equal to or slightly lower than the BSSI. The importance of these values likewise describes a significant factor contributing to tornado probability, intensity, and duration based on the comparison to the BSSI.

The BSSI was interpolated by using existing stationary observations across south-central Kansas, combined with collected mobile surface observations. Other considerations were constructed for storm-scale characteristics and their potential impact to storm inflow. The BSSI was held constant with time, which provides a consistent comparison with time to the derived variables and their associated differences with the base state. A total of 8 minutes within the RFD was collected and broken into two reference frames. The first 4 minutes was north-northeast of the tornado, whereas the final 4 minutes was west-southwest of the tornado. In addition, these reference points were then broken into four quadrants, centered on the tornado centroid, with a radius of 4.5 km. Previous investigations (Markowski et al. 2002) provide a similar example. Due to the spatial and temporal location of sampled observations, only quadrant 1 (Q1) and quadrant 3 (Q3) were considered for analysis.

Θe values collected within the RFD contain much similarity to those of the BSSI. The Θe values calculated for the averaged BSSI was 355.20 K. In contrast, the Θe values calculated for the averaged for the RFD was 354.37 K. This results in an average Θe RFD departure value of 0.83 K cooler than the BSSI. Both Q1 and Q3 contained similar Θe values with 354.35 K and 354.38 K respectively. Θv values found closely resemble those of the BSSI. The Θv values calculated for the averaged BSSI was 307.71 K. In contrast, the Θv values calculated for the averaged for the RFD was 305.44 K. This results in an average Θv RFD departure value of 2.27 K cooler than the BSSI. Q1 and Q3 Θv values were 305.66 K and 305.23 K respectively. It is thought the Θv values in Q1 are closer to the BSSI than Q3 due to the potential entrainment of both RFD origin air potentially mixing with storm inflow. Lastly, CAPE was calculated using data from the LMN 00z upper air sounding and modifying surface values to represent the BSSI and RFD. It was found the BSSI CAPE was on the order of 4050 J Kg^{-1}, whereas the RFD CAPE was 3543 J Kg^{-1}. This results in a departure of 507 J Kg^{-1}. The data suggests the characteristics associated with the RFD were "warm" and buoyant in nature. Such small departures in Θe, Θv, and CAPE have been frequently documented with strongly tornadic supercells (Markowski et al. 2002; Grzych et al. 2004), and it is hypothesized a similar correlation can be applied to sampled data.

6. VISUAL OBSERVATIONS

Visual observations were made by the authors during the time frame before, during, and after the tornado. All observations made during this duration were observed along Kansas Highway 15

(HWY15). The authors remained as close as possible within a safe distance to clearly observe all characteristics of the tornado.

At 0017 UTC, the supercell was classic in nature with a large rotating mesocyclone, rain-free region and striated vault. A wall cloud was present during the entire observation time before tornadogenesis. The precipitation core was located to the north and northeast of the updraft with a thin band of precipitation wrapping to the west side of the mesocyclone. Large hail was observed in an area due north of the mesocyclone. The stones were isolated in occurrence and ranged from 50 - 100 mm.

First signs of imminent tornadic development occurred at 0020 UTC as a pointy funnel cloud developed within the wall cloud. Cyclonic banding on the underside of the mesocyclone appeared to become more pronounced during this time period. At 0021 UTC, the funnel stretched rapidly downward and fully condensed with the ground, signifying the beginning of the tornado 1.6 km southeast of Mulvane, Kansas. The tube expanded slightly and small debris was noted. The tornadic circulation was multi-vortex in nature and appeared to retain this characteristic throughout the entire duration.

As the tornado approached HWY15, the tornado condensation diameter expanded while the bottom of the tornado condensation was not consistent. Still, condensed multiple vortices were frequently observed under the condensed funnel which was lowered eighty percent to the ground. At 0025 UTC, the tornado crossed HWY15 and a moderate amount of debris, both structural and vegetative, was noted within 0.4 km of the authors' location.

At 0026 UTC, the authors crossed the damage path along HWY15 and noted moderate damage 0.45 km wide. At 0027 UTC, substantial multi-vortex organization under the parent condensed cone was observed 4 km southeast of Mulvane, Kansas. Wrap around "hook echo" precipitation moved over the authors' location during this time and significant rear-flank downdraft wind gusts were noted. Lightning activity appeared particular active near the mesocyclone region.

Visible signs of outflow interruption with the tornado occurred at 0029 UTC 4.8 km south of Mulvane, Kansas. The tornado became fully condensed and tilted to the south and forward progression slightly increased. As the tornado tilted more southward, wrap around precipitation began to lessen around the circulation. With a relatively low sun angle and the tilting of the tornado, several optical variables created a highly photogenic and contrasted view due west of the tornado (Fig. 13).

At 0031 UTC, the upper portion of the tornado vortex was orientated nearly horizontal with a relatively abrupt bend oriented vertically 30 degrees toward the south. During this time frame, a "u-shaped" horseshoe vortex (HV) developed in the vicinity of the north side of the tornado bend. It is hypothesized this HV developed in a region of enhanced horizontal vorticity. The HV became stretched from the influence of the tornadic circulation near the bend. It is interesting to note that the southern portion of the HV remained anchored to its origin, whereas the northern portion appeared to vertically accelerate slightly faster than the tornado vertical motion. This feature persisted for a total of 30 seconds before becoming engulfed within the tornadic circulation. Future

investigation of this feature seems plausible given the relatively rare documentation of a HV in association with a tornado.

Shortly after the observed HV, the tornado struck a residential structure 6.4 km southeast of Mulvane, KS, sending a significant amount of large structural debris into the air. The rotational speed appeared to increase as the tornado width slowly constricted. Multi-vortex circulation was highly concentrated in a small width and the motion appeared violent in nature.

The dissipating stage of the tornado was strongly evident at 0032 UTC as the vortex width shrunk. The upper horizontal portion of the tornado slowly lifted vertically and became ingested into the updraft. The rope tornado traversed over a small lake and eventually dissipated leaving a broad dusty rotation in a wheat field 8 km east-southeast of Mulvane, Kansas at 0033 UTC.

7. SUMMARY

The Mulvane, Kansas tornado presented some classic features expected to be observed with most supercells, along with several interesting abnormalities. By examining portions of the storm during varying times in relation to tornadogenesis, several substantial correlations and characteristics were exposed.

It was found that while a large region of the central plains was favorable for supercells and tornadoes, only one small region succeeded in tornado production. Several mesoscale surface boundaries aided in providing a localized region of enhanced strong tornado potential just southeast of Mulvane, Kansas. It is apparent that the internal supercell characteristics combined with these mesoscale surface features assisted greatly in tornadogenesis. Mobile surface observations taken within close proximity of the tornado allowed investigating the surface thermodynamics and kinematics associated with the mesocyclone and tornado. In-depth analysis was preformed on the RFD region to acquire some conception to the properties of this feature. It was found that the RFD associated with the Mulvane, Kansas tornado contained similar thermodynamic values to the BSSI, and therefore was "warm" and buoyant in nature. This is speculated to have enhanced tornado probability, intensity, and duration of this event.

Reflectivity height, related to the BWER and negative charge region in the storm, and the attendant evolution allowed for the production of active lightning strikes near and just south of the surface mesocyclone during a limited duration. Likewise, the coincident strike activity was correlated with updraft strength.

Visual observations by the authors prior, during, and post tornadogenesis served as an important basis for fully comprehending the physical workings of the supercell and tornado. With the ability to fully observe the storm in present state, visual features can be obtained that would otherwise not be documented by remotely sensed methods due to spatial and temporal limitations. In the future, more in-depth analysis will be preformed on the entire supercell duration and concentrate on other smaller tornadoes documented from 12 June 2004.
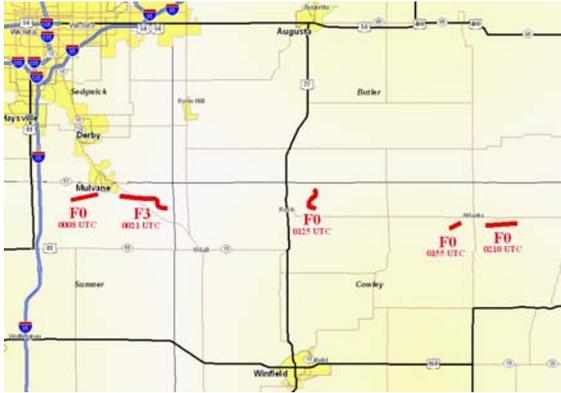
FIGURES

Fig. 1. Tornado paths (red), F-scale ratings, and touchdown times associated with tornadic supercell during 0000 – 0300 UTC.
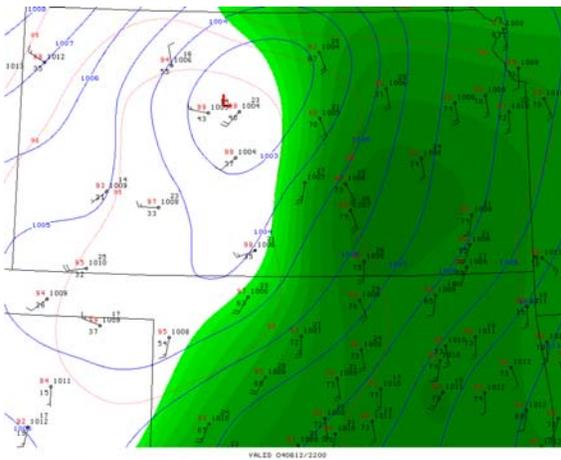

Fig. 2. 2200 UTC surface analysis with isodrosothermal contour. SUP1 initiated along the dryline during this period across southern Kansas.
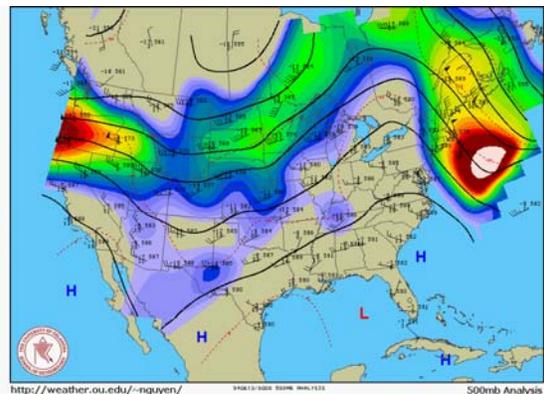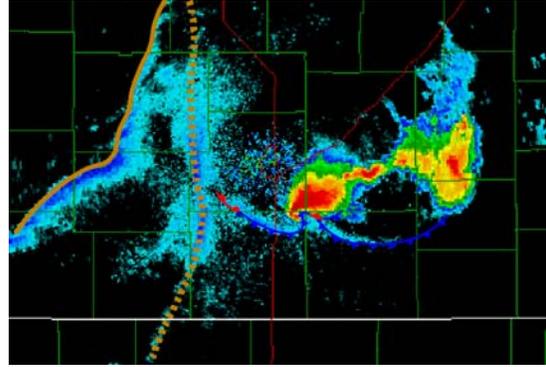

Fig. 3. 500mb 0000 UTC analysis.

Fig. 4. 0027 UTC. Fine line echoes aided in accurate placement of mesoscale features. Dryline (solid brown), confluence line (dashed brown), RFD/FFD/outflow boundary (traditional frontal symbol).
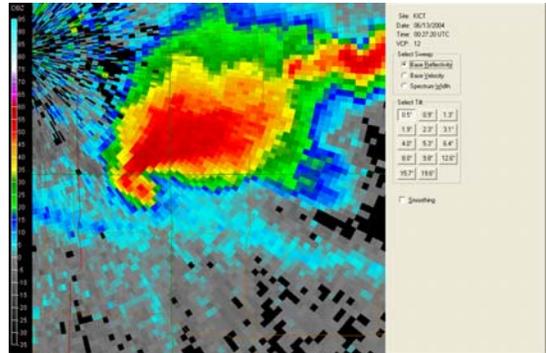

Fig. 5. 0027 UTC base reflectivity image (ICT). Image presents classic supercell characteristics.
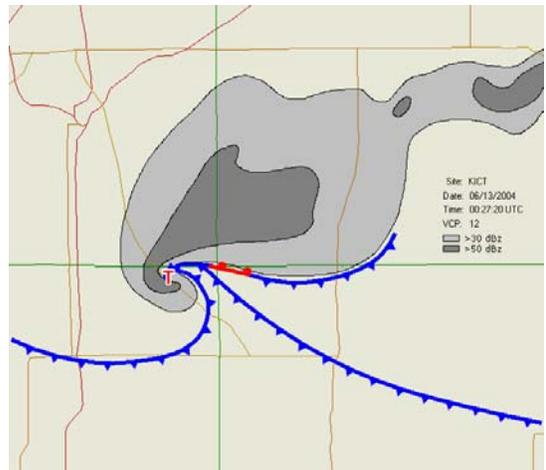

Fig. 6. 0027 UTC storm-scale model showing prominent surface boundaries. "T" demarks location of tornado. dBZ values are in 30 (light grey) and 50 (dark grey) contours.

Fig. 7. Cross-sectional analysis during 0018 UTC. Image shows well-developed BWER region.

Fig. 8. Cross-sectional analysis during 0036 UTC. Image shows partial collapse of the BWER region, leading to a disorganized phase in the supercell.

Fig. 9. Lightning strikes per minute during 0000 – 0059 UTC within a 25 mile radius of the storm centroid.

Fig. 10. Lightning strikes per minute plotted during 0000 – 0059 UTC within a 25 mile radius of the storm centroid. Tornado track (red).

Fig. 11. Mobile surface observations collected during supercell transect 0000 - 0100 UTC (No time-to-space conversions).

Fig. 12. RFD observations averaged per 30 seconds during 00:26:30 – 00:30:30 UTC.

Fig. 13. Mulvane, Kansas tornado. Photo taken (Scott Blair) 0030 UTC, view looking east-southeast.

REFERENCES

Atkins, N. T., M. L. Weisman, and L. J. Wicker, 1999: The influence of preexisting boundaries on supercell evolution. *Mon. Wea. Rev.*, **127**, 2910-2927.

Bluestein, H. B., and D. R. MacGorman, 1998: Evolution of cloud-to-ground lightning characteristics and storm structure in the Spearman, Texas, tornadic supercells of 31 May 1990. *Mon. Wea. Rev.*, **126**, 1451-1467.

Edwards, R., R. L. Thompson, J. G. LaDue, 2000: Initiation of storm A (3 May 1999) along a possible horizontal convective roll. *20th Conf. on Severe Local Storms, Amer. Meteor. Soc., Orlando, FL.*

Finley, C. A., and B. D. Lee, 2004: High resolution mobile mesonet observations of rfd surges in the June 9 Basset, Nebraska supercell during project answers 2003. *22nd Conf. on Severe Local Storms, Amer. Meteor. Soc., Hyannis, MA.*

Grzych, M. L., B. D. Lee, C. A. Finley, and J. L. Schroeder, 2004: Thermodynamic characterization of supercell rear-flank downdrafts in project answers 2003. *22nd Conf. on Severe Local Storms, Amer. Meteor. Soc., Hyannis, MA.*

Lemon, L. R., D. W. Burgess, and R. A. Brown, 1978: Tornadic storm airflow and morphology derived from single-doppler radar measurements. *Mon. Wea. Rev.*, **106**, 48-61.

Lemon, L. R. and C. A. Doswell III, 1979: Severe thunderstorm evolution and mesocyclone structure as related to tornadogenesis. *Mon. Wea. Rev.*, **107**, 1184-1197.

Lindsey, D. T., and M. J. Bunkers, 2004: On the motion and interaction between left- and right-moving supercells on 4 May 2003. *22nd Conf. on Severe Local Storms, Amer. Meteor. Soc., Hyannis, MA.*

MacGorman, D. R., D. W. Burgess, V. Mazur, D. Rust, W. L. Taylor, and B. C. Johnson, 1989: Lightning rates relative to tornadic storm evolution on 22 May 1981. *J. Atmos. Sci.*, **46**, 221-250.

MacGorman, D. R., and K. E. Nielsen, 1991: Cloud-to-ground lightning in a tornadic storm on 8 May 1986. *Mon. Wea. Rev.*, **119**, 1557-1574.

Markowski, P. M., E. N. Rasmussen, and J. M. Straka, 1998: The occurrence of tornadoes in supercells interacting with boundaries during VORTEX-95. *Wea. Forecasting*, **13**, 852-859.

Markowski, P. M., J. M. Straka, and E. N. Rasmussen, 2002: Direct surface thermodynamic observations within the rear-flank downdrafts of nontornadic and tornadic supercells. *Mon. Wea. Rev.*, **130**, 1692-1721.

Perez, A. H., L. J. Wicker, and R. E. Orville, 1997: Characteristics of cloud- to-ground

lightning associated with violent tornadoes. *Wea. Forecasting*, **12**, 428-437.

Straka, J. M., E. N. Rasmussen, and S. E. Fredrickson, 1996: A mobile mesonet for finescale meteorological observations. *J. Atmos. Oceanic Technol.*, **13**, 921-936.